Modelling GCaMP responses: From spikes to fluorescence

Thomas J. Delaney[1], Michael C. Ashby[2], Cian O'Donnell[1]

[1]Department of Computer Science, [2]School of Physiology, Pharmacology and Neuroscience, University of Bristol, UK

Introduction

The use of fluorescent calcium indicators, such as GCaMP6s to monitor neuronal activity is widespread. But the relationship between GCaMP6s fluorescence and action potential firing is poorly understood.

Furthermore, the effects of the indicator characteristics on this fluorescence signal are unknown. For example, it is known that the GCaMP6s indicator accumulates within neurons over weeks and months, which creates difficulties in comparing activity statistics across time-points. As a result, whether or not spike train inference is always possible using GCaMP6s fluorescence remains unknown.

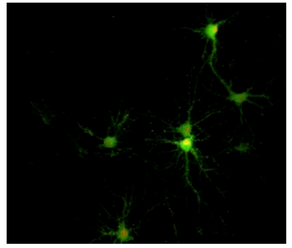

Figure 1: Single frame from video of spontaneous activity recorded from cultured mouse hippocampal neurons using GCaMP6s fluorescent indicator. Image courtesy of brainslicemethods.com

Aims

- To simulate the fluorescence traces produced by a fluorescent calcium indicator in a neuron soma.
- To understand how indicator characteristics affect fluorescence signal-to-noise ratio and the quality of spike train inference.
- To facilitate benchmarking of the various spike inference algorithms that have recently been developed.

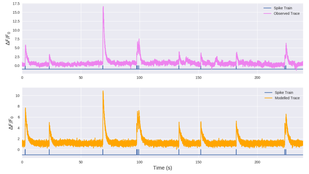

Figure 2: The violet trace is the observed fluorescence from the primary visual cortex in an anesthetized mouse watching a drifting grating movie. The spike train was measured simultaneously using electrophysiological methods.
The orange trace is produced by the fluorescent indicator model after parameter calibration.

Methods

- We modelled five dynamic variables, the concentrations of:
  - Free calcium ions,
  - Fluorescent indicator proteins,
  - Mobile endogeneous buffers,
  - Immobile endogeneous buffers,
  - Excited indicator bound calcium molecules.

  These were modelled using a system of first order ODEs. The equations modelled reactions similar to that of the fluorescent indicator and calcium reactions described above, except without the photon dynamics.
- Action potentials were modelled by an instantaneous jump in the concentration of free calcium ions.
- Collecting the released photons was modelled as a random variable with binomial distribution.

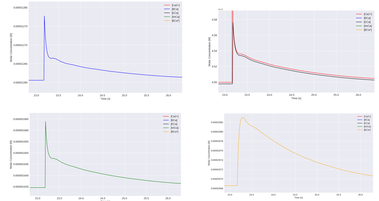

Figure 3: Dynamics of indicator bound calcium concentration [BCa], endogeneous mobile bound calcium concentration [ECa], endogeneous immobile bound calcium concentration [ImCa], and excited indicator bound calcium concentration around one action potential (top left, top right, bottom left, bottom right respectively).

Two-photon imaging with fluorescent calcium indicators

When an action potential is fired by a neuron, the concentration of free calcium $[Ca^{2+}]$ within the neuron increases rapidly, and decays relatively slowly. These calcium ions bind to proteins within the neuron cytoplasm called *buffers* [B]. The fluorescent indicator is another one of these buffers, with the special property that the indicator bound calcium molecules can fluoresce (release a photon).

$$[B][Ca^{2+}] \underset{b}{\overset{f}{\rightleftharpoons}} [BCa] \rightsquigarrow [BCa^*]$$

In two-photon imaging, fluorescent indicator is inserted into a piece of brain tissue either by injection, transportation by a virus, or expression from genetically modified neurons. Photons are then fired at the target piece of tissue. If one of the indicator bound calcium molecules [BCa] is excited by these photons, the molecule will release another photon in turn. The photons released by the [BCa] molecules can then be used to form an image of the tissue showing the neurons.

Fitting Free Parameters

Our model of the calcium and fluorescence dynamics has four free parameters:

Calcium rate, β This is the rate at which the $[Ca^{2+}]$ concentration is driven back to the baseline [3] concentration level.

Excitation rate, ϵ This defines how many indicator bound calcium molecules become excited by photon bombardment per second.

Release rate, r This defines how many excited indicator bound calcium molecules will release a photon and go back to their relaxed state per second.

Capture rate, p This defines the probability of a photon detector capturing a photon released by an excited indicator bound calcium molecule. It is essentially the p parameter of the binomial distribution used to model the photon capture process.

The optimal values for the free parameters were found using a suite of stochastic optimisation algorithms. The objective function was the sum of the root-mean-squared difference between the observed fluorescence trace and the modelled fluorescence trace and the root-mean-squared difference between the smoothed power spectra of the observed fluorescence trace and the modelled fluorescence trace. The lower the value of the objective function, the better the optimisation.

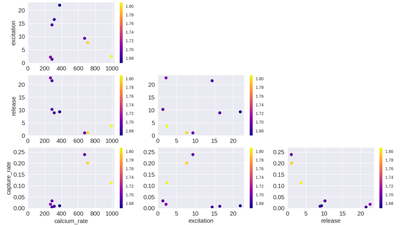

Figure 4: Relationships between optimised free parameters for a given trace. Each data point corresponds to a set of optimised free parameters from one of the seven optimisation algorithms that were applied to the traces. The deep blue points are the better optimised points, the worse optimisations are in yellow.

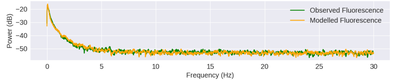

Figure 5: The log power spectrum of an observed fluorescence trace, and a modelled fluorescence trace after the fitting procedure.

julia

Perturbing parameters

- We varied the parameters of the model and created fluorescence traces.
- We measured the signal-to-noise ratio of the traces, using the perturbed and experimental values. We used the ratio of the mean $\Delta F/F_0$ to the mean noise σ in the fluorescence trace as the definition of the SNR.
- Then we used a deconvolution algorithm [1] to infer spike trains from these traces. We measured the quality of the inference using the *true-positive rate*, aka. the *recall* or *hit-rate*.

Varying the fluorescent calcium indicator concentration

We perturbed the concentration of the fluorescent calcium indicator within the cell soma around the experimental value in order to assess the effect on fluorescence. We used four perturbed values, two higher and two lower.

The higher and lower perturbations affected the fluorescence traces in different ways. But for the more extreme perturbations, the SNR ratio decreased and the inference quality decreased either way.

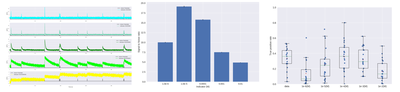

Figure 6: (left) An example trace for each of the five perturbed values for the concentration of fluorescent calcium indicator. The top two traces are produced by the lower perturbed values, the middle trace is produced by the experimental value, and the lowest two traces are produced when using the higher perturbed values.
(middle) The signal-to-noise ratio of the modelled fluorescence traces using each of the four perturbed values, and the experimental value. Extreme perturbations of the concentration either above or below the experimental level lowered the SNR.
(right) The true-positive rates of the deconvolution algorithm's predictions when inferring from the observed data, and inferring from modelled traces using the perturbed and experimental values. We found that the algorithms performs equally badly on the two most extreme values, and performs equally well on the experimental value, and the next higher perturbed value.

Varying the immobile endogeneous buffer concentration

We perturbed the concentration of the immobile endogeneous buffer around the experimental value in order to asses the effects of different levels of immobile buffer on the fluorescence traces.

Having less immobile endogeneous buffer had little effect. But having more immobile buffer caused a smaller change in fluorescence due to an action potential, and a slower decay in fluorescence. The signal-to-noise ratio was also smaller for higher values of immobile buffer as a result.

Varying the immobile endogeneous buffer concentration

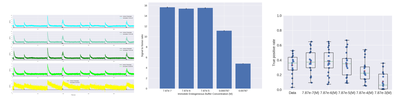

Figure 7: (left) An example trace for each of the five perturbed values for the concentration of immobile endogeneous buffer.
(middle) The signal-to-noise ratio of the modelled fluorescence traces using each of the four perturbed values, and the experimental value. The lower values for the immobile buffer produce the same SNR as the experimental value. But the higher perturbed values produce fluorescence traces with a lower SNR.
(right) The true-positive rates of the deconvolution algorithm's predictions when inferring from the observed data, and inferring from modelled traces using the perturbed and experimental values.

Varying indicator binding and unbinding rates

We varied the binding and unbinding rates of the fluorescent calcium indicator. But we varied these values proportionally so that their ratio, the dissociation constant, was the same for all perturbations.

We found that when the lower perturbed values for the rates are used the change in fluorescence due to an action potential is smaller, and therefore the signal-to-noise ratio is lower. We also found this result reflected in the quality of spike inference from the traces produced using the lower perturbed values.

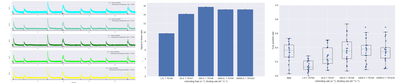

Figure 8: (left) An example trace for each of the five pairs of values used for the binding and unbinding rates of the fluorescent calcium indicator.
(middle) The signal-to-noise ratio of the modelled fluorescence traces using each of the four perturbed values, and the experimental value. The SNRs for the two pairs with values lower than the experimental value are lower than the experimental pair or the higher value pairs.
(right) The true-positive rates of the deconvolution algorithm's predictions when inferring from the observed data, and inferring from modelled traces using the perturbed and experimental values.

Limitations

The are a number of limitations to our model. For a start, the equations that define the model do not attempt to model the binding dynamics of calcium buffers such as calmodulin. Specifically, the cooperative or antagonistic pairing between binding sites is not included.

Secondly, there are dozens of different mobile and immobile endogeneous buffers with different association and dissociation rates. Here, we have lumped these buffers together into two modelled concentrations.

Lastly, in this model we have assumed that the indicator bound calcium molecules are constantly under photon bombardment. But in reality, a laser systematically scans across the tissue, exciting molecules as it goes along.

Conclusion

- We varied the parameters of the model and measured the effect of these variations on the signal to noise ratio of the modelled traces, and the quality of the spike inference. We found that variations in the fluorescent calcium indicator affects the modelled traces, SNR, and spike inference in different ways.
- We found that increasing the concentration of immobile endogeneous buffer increased the decay time of the fluorescence traces, decreased the SNR, and decreased the quality of spike inference.
- Finally we found that decreasing both the unbinding and binding rates of the fluorescent calcium indicator simultaneously decreases the SNR, and decreases the quality of spike inference.
- The parameters of the model can be calibrated to those of different fluorescent indicators, and the any spike train can be used as an input to the model. Therefore, our intention is that this model could be used by researchers to simulate the appearance or characteristics of fluorescence traces under their own specific experimental circumstances. This could help researchers to choose a more suitable indicator, or to assess the challenges associated with using a fluorescent calcium indicator.

References

[1] E.A. Pnevmatikakis, D. Soudry, Y. Gao, T.A. Machado, J. Merel, D. Pfau, T. Reardon, Y. Mu, C. Lacefield, W. Yang, M. Ahrens, R. Bruno, T.M. Jessell, D.S. Peterka, R.Yuste, L. Paninski *Simultaneous Denoising, Deconvolution, and Demixing of Calcium Imaging Data*, Neuron 89, 285-299, (2016)

[2] Tsai-Wen Chen, Trevor J. Wardill, Yi Sun, Stefan R. Pulver, Sabine L. Renninger, Amy Baohan, Eric R. Schreiter, Rex A. Kerr, Michael B. Orger, Vivek Jayaraman, Loren L. Looger, Karel Svoboda, Douglas S. Kim, *Ultrasensitive fluorescent proteins for imaging neuronal activity*. Nature 499, 295-300, (2013)

[3] M. Maravall, Z. F. Mainen, B. L. Sabatini, K. Svoboda, *Estimating intracellular calcium concentrations and buffering without wavelength ratioing*. Biophysical Journal 78, 2655-2667, (2000)

Acknowledgements

I would like to thank Conor Houghton for his help in preparing this poster. This is an EPSRC funded project.

Contact Information

- Web: http://www.bristol.ac.uk/engineering/research/computational-neuroscience/
- Email: t.delaney@bristol.ac.uk
- Address: 81-83 Woodland Road,
  University of Bristol,
  Bristol,
  BS3 1US,
  UK